

# SHIFTING BOUNDARIES: ECOLOGICAL AND GEOGRAPHICAL RANGE EXTENSION BASED ON THREE NEW SPECIES IN THE CYANOBACTERIAL GENERA *CYANOCOHNIELLA*, *OCULATELLA*, AND *ALITERELLA*<sup>1</sup>

Patrick Jung <sup>2</sup>

University of Applied Sciences Kaiserslautern, Carl-Schurz-Str. 10-16, 66953 Pirmasens, Germany

Tatiana Mikhailyuk 

G. Kholodny Institute of Botany, National Academy of Sciences of Ukraine, Tereshchenkivska Str. 2, Kyiv 01004, Ukraine

Dina Emrich


Faculty of Environment and Natural Resources, Chair of Applied Vegetation Ecology, University of Freiburg, Tennenbacher Str. 4, 79106 Freiburg, Germany

Karen Baumann 

Faculty of Agricultural and Environmental Science, University of Rostock, Soil Science, Justus-von-Liebig-Weg 6, 18051 Rostock, Germany

Stefan Dultz

Institute of Soil Science, Leibniz Universität Hannover, Herrenhäuser Str. 2, 30419 Hannover, Germany

and Burkhard Büdel 

Plant Ecology and Systematics, University of Kaiserslautern, Erwin-Schrödinger-Str. 13, 67663 Kaiserslautern, Germany

The polyphasic approach has been widely applied in cyanobacterial taxonomy, which frequently led to additions to the species inventory. Increasing our knowledge about species and the habitats they were isolated from enables new insights into the ecology of newly established genera and species allowing speculations about the ecological niche of taxa. Here, we are describing three new species belonging to three genera that broadens the ecological amplitude and the geographical range of each of the three genera. *Cyanocohniella crotaloides* sp. nov. is described from sandy beach mats of the temperate island Schiermonnikoog, Netherlands, *Oculatella crustae-formantes* sp. nov. was isolated from biological soil crusts of the Arctic Spitsbergen, Norway, and *Aliterella chasmolithica* originated from granitic stones of the arid Atacama Desert, Chile. All three species could be separated from related species using molecular sequencing of the 16S rRNA gene and 16S–23S ITS gene region, the resulting secondary structures as well as p-distance analyses of the 16S–23S ITS and various microscopic techniques. The novel taxa described in

this study contribute to a better understanding of the diversity of the genera *Cyanocohniella*, *Oculatella*, and *Aliterella* in different habitats.

**Key index words:** 16-23S ITS; Atacama Desert; polyphasic approach; Schiermonnikoog; Spitsbergen

**Abbreviations:** a.s.l., above sea level

<sup>1</sup>Received 23 August 2019. Accepted 28 March 2020. Published Online 27 June 2020, Wiley Online Library (wileyonlinelibrary.com).

<sup>2</sup>Author for correspondence: e-mail patrick\_jung90@web.de.

Editorial Responsibility: J. Collier (Associate Editor)

Cyanobacteria are considered the most ancient and ecologically important group of oxygenic photosynthetic microorganisms that has significantly influenced the history of the Earth (Whitton 2012). Nevertheless, their taxonomic resolution has been historically challenging due to taxonomically uninformative characteristics and the nescience about their ecological niche. For example, the sole use of micromorphological features obtained by microscopy as applied in the past is currently considered insufficient for the definition of genera and species (Taton et al. 2003, Komárek 2006, Engene et al. 2010). Instead, phylogenies based on the 16S rRNA gene and 16S–23S ITS region, including secondary structures, are currently widely used for generic definitions as they are more reliable (Komárek et al. 2014). Recently, the p-distances between aligned ITS sequences were used as additional evidence for species recognition and this has been so far

consistent with recognition of near-cryptic to cryptic taxa (e.g., Shalygin et al. 2019, Vázquez-Martínez et al. 2018, González-Resendiz et al. 2019). Therefore, cyanobacterial taxonomy is now combining molecular, ecological, and morphological data, thus forming the so-called ‘polyphasic approach’ (Johansen and Casamatta 2005). This approach has widely been established leading to an extensive revision of the classification system during the last decade (Komárek et al. 2014).

In 2012, for example, based on phylogenetic and morphological evidences, Zammit et al. (2012) separated the genus *Oculatella* from the filamentous, non-heterocytous genus *Leptolyngbya*, one of the morphologically most poorly defined genera due to their faintly differentiated trichome morphology. The morphotype of the genus *Oculatella* was first reported in 1988 by Albertano and Grilli-Caiola and later described as *Leptolyngbya* ‘Albertano/Kováčik-red’ (Komárek and Anagnostidis 2005). This seems surprising since the *Leptolyngbya* isolate is actually unique compared to other *Leptolyngbya* species, based on the rhodopsin-like reddish inclusion at the tip of mature apical cells (Albertano et al. 2000), a feature that has now become the main characteristic of the whole genus *Oculatella* (Zammit et al. 2012). Only a few other species within the genus *Oculatella* have been described since the first description (Osorio-Santos et al. 2014, Vinogradova et al. 2017).

The type species *Oculatella subterranea* has been reported from caves in the Mediterranean region, including Italy, Spain, Malta, and Israel (Albertano and Grilli Caiola 1988, Zammit et al. 2008a,b, 2011, 2012, Martínez and Asencio 2010, Osorio-Santos et al. 2014). Subsequent species were described from arid soils in Greece, the Atacama Desert, and the Mojave Desert (*O. neakameniensis*, *O. atacemensis*, *O. mojaviensis*, *O. coburnii*), a waterfall in Utah (*O. cataractarum*), a German lake (*O. hafneriensis*; see Osorio-Santos et al. 2014 for these species), a sea cave in Kauai (*O. kauaiensis*; Miscoe et al. 2016), and maritime sand dunes (*O. kazantipica*, *O. ucrainica*; Vinogradova et al. 2017). The wide variety of habitats leads to the question of the ecological range of the genus *Oculatella*.

A comparable situation is found in the recently established genus *Cyanocohniella* within the family of the filamentous and heterocytous *Aphanizomenonaceae* with *C. calida* as the only species (Kaštrovský et al. 2014). This species was isolated already in 1863 from thermal springs of Karlovy Vary (Carlsbad), Czech Republic, and was initially described as *Mastigocladus laminosus* f. *nostocoides*. Later, the strain got lost and was re-isolated and finally described as *C. calida* (Kaštrovský et al. 2014). Due to its origin from thermal water >55°C, the species and potentially the whole genus was considered thermophilic (Kaštrovský et al. 2014). Interestingly, the species shows one of the most complex life

cycles known for cyanobacteria, ranging from a *Pseudanabaena/Leptolyngbya*-like stage over a *Nostoc*-like stage to a *Chlorogloeopsis*-like stage causing problems during microscopic investigations of environmental samples.

In contrast to morphologically distinct heterocytous cyanobacteria, coccoid unicellular species such as the recently established genus *Aliterella* lack even more morphological characters (Rigonato et al. 2016). This genus comprises the three aquatic species *A. atlantica*, isolated from the water column of the Atlantic close to south-east Brazil, *A. antarctica*, found in a green turf alga from coastal Antarctica (Rigonato et al. 2016), and finally *A. shaanxiensis* isolated from water samples of a freshwater inland lake in Shaanxi, China (Zhang et al. 2018).

Trying to determine whether a cyanobacterial species is strictly assigned to a specific habitat and/or geographical range is part of understanding its ecology. However, in the past this could only be questionably achieved for a specific species as it was possible that it might also be found in a completely different geographic location or habitat which just had not been investigated yet. Recently, the supposed endemism for originally geographically isolated species such as the Antarctic species *Wilmottia murrayi* (Strunecký et al. 2011) has been challenged based on sequences of the genus with high 16S rRNA genetic identities (99–100%) from China, USA, Spain, Bolivia, New Zealand, and Ireland (Pessi et al. 2018). In contrast, for other species such as *Kastovskya adunca* (Mühlsteinová et al. 2014) from soils of the Atacama Desert the concept of endemism and even substrate specificity can still be applied.

Aiming for a better understanding of the three cyanobacterial genera *Aliterella* (unicellular, aquatic), *Oculatella* (filamentous, non-heterocytous, mostly terrestrial or subaerial habitats), and *Cyanocohniella* (filamentous, heterocytous, thermophilic), the present study reports and describes a new species for each of the three genera, extending their ecological and geographical range. Using molecular sequencing of the 16S rRNA gene and 16S–23S ITS gene region, the resulting secondary structures and p-distance analyses of the 16S–23S ITS as well as various microscopic techniques, we describe three new species: *Aliterella chasmolithica* sp. nov. from chasmolithic biofilms of the Atacama Desert, *Cyanocohniella crotaloides* sp. nov. from algal mats occurring in front of the dune dyke at the North Sea barrier island Schiermonnikoog and *Oculatella crustaeformantes* sp. nov. from biological soil crusts from the Arctic Spitsbergen.

#### MATERIALS AND METHODS

**Sampling sites.** *Spitsbergen:* Soil samples of the top centimeter were taken by Laura Briegel-Williams during August 2014 at Arctic Spitsbergen (Fig. 1A) within an area called Geopol

(78°56'58.38" N, 11°28'35.64" E) where polygon formation dominates skeletal soils. The biome is polar tundra with 4.5°C as the average temperature and 471 mm average precipitation occurring mainly from October to May when the snow cover is complete (based on data from the Norwegian Meteorological Institute). High coverage rates of cryptogams dominated by cyanobacteria were reported for this location (Williams et al. 2017) with *Leptolyngbya antarctica*, *Microcoleus vaginatus*, and several *Nostoc* species as well as the *Oculatella* strain PJ S28 (Jung et al. 2019a) described here.

**Barrier Island Schiermonnikoog:** Samples were collected in May 2018 at mats from the lowest part of the supratidal to the upper part of the intertidal zone of the sandy beaches (53°28'23.62" N, 6°8'32.47" E) of the North Sea barrier island Schiermonnikoog (Fig. 1B). The beach has a typical hydrological zonation with an upper saline plume, terrestrial groundwater discharge from the island aquifer, and a saltwater wedge (Robinson et al. 2007). The climate can be described as warm temperate with 8.6°C as the mean average temperature and 806 mm average precipitation (based on Climate-Data.org). The sandy tidal sediments located at the north-western part of the island are well-sorted grains between 100 and 200  $\mu\text{m}$  diameter and consists mainly of quartz, feldspars, heavy minerals, and <1% carbonates arising from seashells; they are infested by microbial mats that cover an area of more than 7 km<sup>2</sup> (Kremer et al. 2008). Among the ephemeral seasonal microbial community, phototrophic organisms such as *Coleofasciculus chtonoplastes*, *Leptolyngbya aestuarii*, *Spirulina* sp., *Phormidium* sp., and several *Nodularia* species were found to be the most dominant organisms (Bauersachs et al. 2011). The mats are influenced by seawater during high tide as well as by rain, storms, floods, upwelling freshwater, and ice covers. They sporadically lead to the destruction of the microbial mats that form throughout the year.

**Atacama Desert:** The National Park Pan de Azúcar is situated in the northern part of the Atacama Desert, Chile (Fig. 1C), and represents a fog oasis. The climate can be considered as arid with 16.2°C as the mean average temperature and 14.7 mm of mean average precipitation (Baumann et al. 2018) with fog and dew as the main regular water sources (Lehnert et al. 2018). The samples were taken in July 2017, 15 km away from the coast (26°06'39.62" S, 70°32'54.51" W) where no vegetation was observed as described in Jung et al. (2019b). From this area, only a few cyanobacteria such as *Kastovskya adunca*, *Pleurocapsa minor*, *Chroococcidiopsis* sp., *Pseudophormidium* sp., *Nostoc* sp., and others have been reported to appear in the desert soil or aridisol and as hypolithic and chasmoendolithic biofilms attached to exposed granite and quartz boulders (Jung et al. 2019b). The chasmoendolithic *Aliterella* strain PJ S15 discussed here was isolated from granite boulders (Jung et al. 2019b).

**Culture conditions.** The three strains *Cyanocohniella* sp. PJ S45, *Oculatella* sp. PJ S28, and *Aliterella* sp. PJ S15 were isolated by the procedure described in detail by Jung et al. (2019a). In short, solidified Bold's Basal Medium (BBM; Bischof and Bold 1963) was used for enrichment cultures which were incubated in a culture cabinet at 15–17°C under a light:dark regime of 14:10 h at a light intensity of about 20–50  $\mu\text{mol photons} \cdot \text{m}^{-2} \cdot \text{s}^{-1}$  for at least 4 weeks as described in Langhans et al. (2009). The cultures were inspected several times a week for the appearance of cyanobacteria and colonies were transferred with a sterile metal needle to BG11 medium agar plates (Stanier et al. 1971). This was repeated until unialgal cultures were achieved. Subcultures were generated by further serial transfers under sterile conditions to exclude contamination with other cyanobacteria, green algae, or fungi until unialgal isolates could be established.

**Morphological characterization.** The morphology of the three isolates was checked weekly using light microscopy with oil

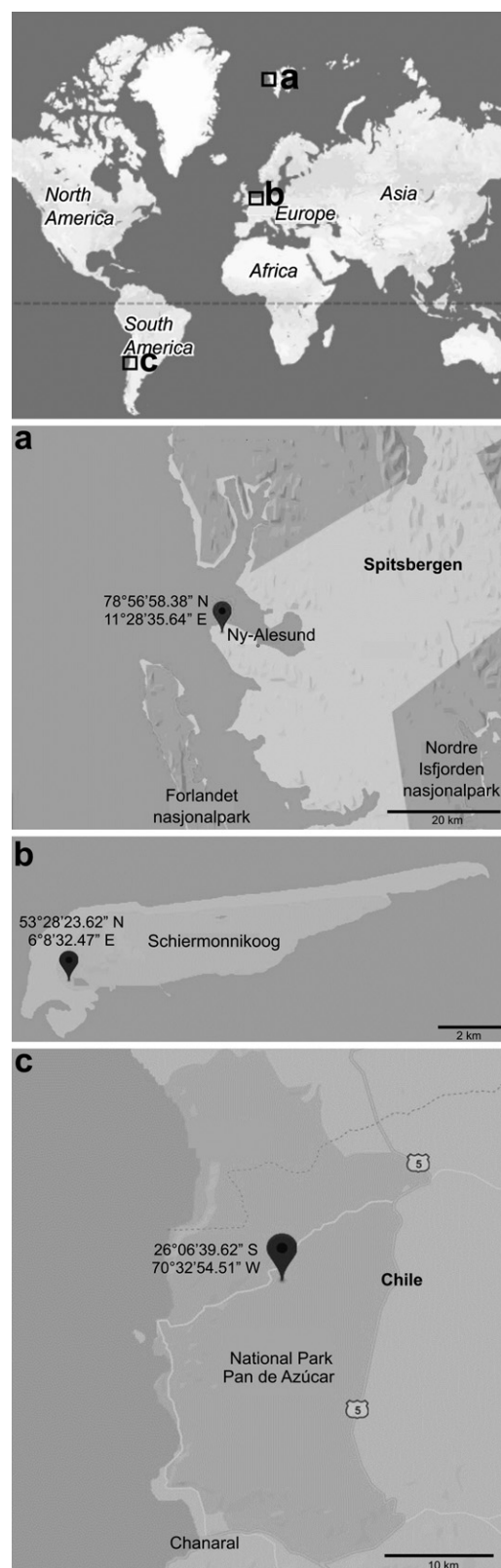


FIG. 1. Overview map of sampling sites. (a) Geopol at Spitsbergen in the Arctic. (b) the Dutch North Sea with barrier island Schiermonnikoog. (c) National Park Pan de Azúcar within the Atacama Desert of Chile. Maps were created using snazzymaps.com.

immersion and a 630-fold magnification (Axioskop; Carl Zeiss) and AxioVision software (Carl Zeiss).

Fifty images were taken from each strain and trichome diameters as well as the length and widths of the cells were measured for 100 cells with ImageJ 1.47v. In the case of *Cyanocohniella* sp., cell sizes are given for the *Nostoc*-like stage because this represents the dominant growth form of the strain. The percentage of apical cells with a red tip from *Oculatella* sp. PJ S28 was determined using presence or absence of a red tip.

In addition, confocal laser scanning microscopy (CLSM) was applied to investigate the position of the thylakoids. For this, small portions of the isolates were transferred to a drop of water on an objective slide before inspected with a CLSM microscope (LSM 700; Carl Zeiss). The CLSM was equipped with diode lasers and photomultiplier parameters were adjusted to achieve the maximum signal from the autofluorescence using beams of 639 nm wavelengths, oil immersion, and a 630-fold magnification. Emitted wavelengths were collected using a band-pass filter 530/30. Cyanobacterial natural fluorescence was collected using a 590-nm-long pass filter. Stack series comprising 30 single images with a distance of 1  $\mu$ m were scanned through the samples of the cross sections and their maximum projection was converted into 2-D pictures using ImageJ 1.47v software.

**DNA extraction, amplification, and sequencing.** Genomic DNA of each strain was extracted from unialgal cultures as described by Jung et al. (2019b). Nucleotide sequences of the 16S rRNA gene together with the 16S–23S ITS region (1,700–2,300 bases) were amplified as described by Marin et al. (2005) using the primers SSU-4-forw and ptLSU C-D-rev. The PCR products were cleaned using the NucleSpin® Gel and PCR Clean-up Kit (Macherey-Nagel GmbH & Co. KG) following the DNA and PCR clean up protocol. The cleaned PCR products were sent to Seq-It GmbH & Co. KG (Pfaffplatz 10, 67655 Kaiserslautern, Germany) for Sanger sequencing with the primers SSU-4-for, Wil 6, Wil 12, Wil 14, Wil 5, Wil 9, Wil 16, and ptLSU C-D-rev (Wilmutte et al. 1993, Marin et al. 2005, Mikhailyuk et al. 2016). The generated sequences were assembled and manually edited where appropriate using the software Mega X (version 10.0.5; Kumar et al. 2018). The sequences were submitted at NCBI GenBank and can be found under the accession numbers MN243147 (*Oculatella crustae-formantes* PJ S28), MN243143 (*Cyanocohniella crotaloides* PJ S45), and MN243145 (*Aliterella chasmolithica* PJ S15).

**Molecular characterization.** The sequences were BLASTed against the GenBank database in order to find the most similar sequences which were subsequently incorporated into each alignment. One alignment for each strain with *Gloeobacter violaceus* PCC 7421 as root was prepared applying the ClustalW algorithm for all alignments in Mega X. Finally, 110 nucleotide sequences for the phylogenetic comparison of *Oculatella* sp. PJ S28 (1,164 bp), 52 for *Cyanocohniella* sp. PJ S45 (1,264 bp), and 54 for *Aliterella* sp. PJ S15 (1,285 bp) were used. Ambiguous regions within each alignment were adjusted or removed manually allowing smaller final blocks and gap positions within the final blocks. The evolutionary model that was best suited to the used database was selected on the basis of the lowest AIC value and calculated in Mega X. Phylogenetic trees were constructed with Mega X using the evolutionary model GTR+G+I model of nucleotide substitutions for the alignment which was previously determined as best model calculated by Mega X for each alignment. The Maximum Likelihood method (ML) with 1,000 bootstrap replications was calculated for each alignment with Mega X as well as Bayesian phylogenetic analyses with two runs of eight Markov chains were executed for one million generations with default parameters with Mr. Bayes 3.2.1 (Ronquist and Huelsenbeck 2003).

In some cases, the 16S phylogeny of cyanobacteria can appear ambiguous for differentiating species, which was recently demonstrated for, for example, the genus *Desertifilum* (González-Resendiz et al. 2019). As an additional concept, percent dissimilarity among aligned 16S–23S ITS regions was displayed by calculating  $100 \times$  uncorrected p-distance in Mega X (Erwin and Thacker 2008, Shalygin et al. 2019, González-Resendiz et al. 2019). The idea behind that is to have a discontinuity between percent dissimilarity of populations in the same species (average  $\sim 1.0\%$  or less, all pair-wise comparisons  $< 3\%$  dissimilarity) and populations representing separate species ( $> 7\%$  dissimilarity; González-Resendiz et al. 2019). When differences are between 3% and 7%, the cut-off is not clear and a decision can be based on the other criteria such as 16S phylogeny or morphology.

Models of the secondary structure of 16S–23S ITS region of *Oculatella* sp. PJ S28 (D1–D1', Box-B, V2, and V3 helices), *Cyanocohniella* sp. PJ S45 (D1–D1', Box-B, and V3 helices), and *Aliterella* sp. PJ S15 (D1–D1' and Box-B helices) in comparison with several known species were built according to the models proposed in respective papers (Osorio-Santos et al. 2014, Kaštovský et al. 2014, Vinogradova et al. 2017, Zhang et al. 2018). Helices were folded with the online software Mfold (Zuker 2003) and visualized in the online tool PseudoViewer (Byun and Han 2009).

**Toxin characterization.** Extracted genomic DNA of the three strains was used to test potential ability of the cyanobacteria to synthesize microcystin and nodularin. The primer pair HEPF/R targeting the *mcyE/ndaF* gene was used (Jungblut and Neilan 2006) as described by Gehring et al. 2012.

**Strains, herbarium specimens, and accession numbers.** The three cyanobacterial strains were deposited at the German Collection for Microorganisms and Cell Cultures DSMZ Braunschweig, Germany, as well as the culture collection SAG of Göttingen, Germany. The generated sequences were deposited in GenBank and can be found under the accession numbers MN243147 (*Oculatella crustae-formantes* PJ S28), MN243143 (*Cyanocohniella crotaloides* PJ S45), and MN243145 (*Aliterella chasmolithica* PJ S15). From the cultures, herbarium specimens were prepared. Species were described following the rules and requirements of the International Code of Nomenclature for algae, fungi, and plants (Turland et al. 2018). Furthermore young (3 weeks old) cultures were preserved in 4% formaldehyde, in 15-mL glass bottles. Preserved material was then deposited in the Herbarium Hamburgense, Hamburg, Germany.

## RESULTS

Each of the three investigated cyanobacterial strains was found to be unique based on its ecology, morphology, distribution, phylogeny, p-distance analysis of the 16S–23S ITS, and secondary structures. Because the combination of diacritical features associated with these species did not correspond with any described species of each of the three genera, we here named the three strains as the new species *Aliterella chasmolithica* sp. nov., *Oculatella crustae-formantes* sp. nov., and *Cyanocohniella crotaloides* sp. nov.

***Cyanocohniella crotaloides* P. Jung, Mikhailyuk, Emrich, Dultz et Büdel sp. nov. (Fig. 2, Table 1).**

**Description:** Populations of *Cyanocohniella crotaloides* sp. nov. show a polymorphic life cycle. The adult and main form resembles those of *Nostoc*-like

thallus structures with curved, constricted filaments that are embedded in a nonlamellated, fine and colorless sheath. The cells are round to spherical, 2.1–3.7  $\mu\text{m}$  in diameter, with parietal thylakoids, and rarely with intercalary oval to spherical heterocysts. Young filaments or motile hormogonia show a *Pseudanabaena*/*Leptolyngbya*-like morphology with constricted cells that are cylindrical and 1.5–3.1  $\mu\text{m}$  wide. The apical cells of these filaments are longer than wide, 1.5–3.1  $\mu\text{m}$ , and oval to conical. Mature filaments resemble a *Chlorogloeopsis*-like morphology with cells of different sizes in one trichome formed by cell division in two planes. The cells are spherical, oval, or irregularly shaped and vary from 2.6 to 5  $\mu\text{m}$ . The filaments are ensheathed in a visible, firm, and colorless sheath with apical and multiple intercalary hormocytes. Akinetes are formed in this stage and stayed attached to the filaments as single cells or in series with a brownish color. The cells are spherical to oval, 2.8–6.3  $\mu\text{m}$  in diameter. The species tested negatively for nodularin/microcystin genes.

**Habitat:** Beach mats.

**Etymology:** ‘*Crotaloides*’ according to the rattlesnake-like habit of the *Chlorogloeopsis*-like stage where variable cell types and cell sizes are combined and look like a rattle.

**Type locality:** -NETHERLANDS. Schiermonnikoog island, North Sea: beach mats formed of fine sands, elev. 2 m, 53°28'23.62" N, 6°8'32.472" E, collected on 24.05.2018, and isolated by P. Jung.

**Holotype:** The preserved holotype specimen is available via the Herbarium Hamburgense, Hamburg, Germany (HBG024670). It was prepared from the living strain which was the source of 16S, ITS, and 23S rRNA gene sequence deposited as GenBank accession number MN243143.

**Reference strain:** The reference strain is available via the culture collection DSMZ Braunschweig (DSM 109255) and the culture collection SAG of Göttingen, Germany (SAG 2592).

**Phylogenetic relations and secondary structure of the 16S–23S ITS:** A total of 52 sequences of representative taxa were included in the phylogenetic analyses to assess the placement of the *Cyanocohniella* clade in the Cyanobacteria (Fig. 2A). ML and Bayesian inference analyses produced similar tree topologies in our phylogenies. *Cyanocohniella crotaloides* sp. nov. is highly related to *C. calida* (99.9%) with one nucleotide difference in the 16S rRNA (Table S1 in the Supporting Information), but shows great differences (12.7%) in the p-distance of 16-23S ITS rRNA gene (Table S2 in the Supporting Information). The species shows major differences

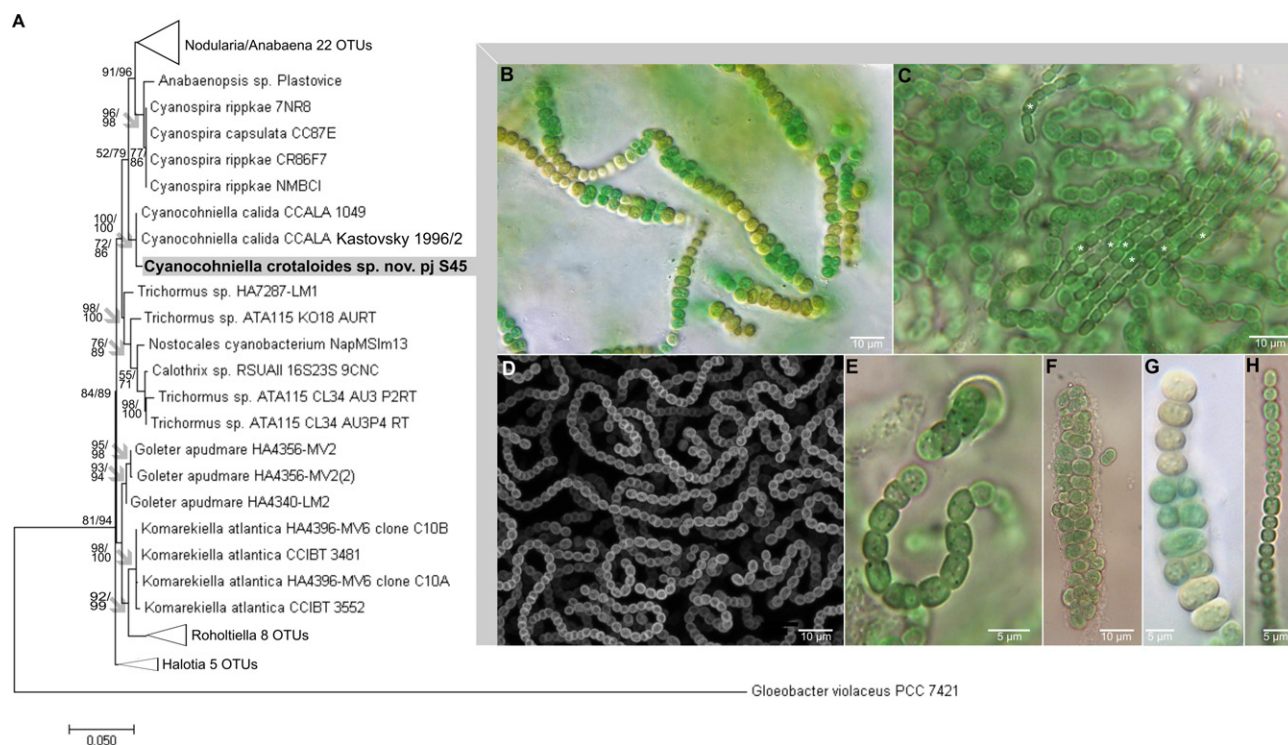


FIG. 2. Phylogenetic tree and micrographs of *Cyanocohniella crotaloides* sp. nov. (A) Phylogenetic position of *Cyanocohniella crotaloides* sp. nov. based on the 16S rRNA gene sequence data rooted to *Gloeobacter violaceus* PCC 7421. Numbers at nodes represent first the ML bootstrap support (values  $\geq 50\%$ ) and second the posterior probabilities from the Bayesian analysis (values  $\geq 50\%$ ). The scale indicates the numbers of substitutions per site. (B) *Chlorogloeopsis*-like stage with brownish akinetes and different cell sizes in one trichome and multiple branching. (C) *Nostoc*-like stage with *Pseudanabaena*/*Leptolyngbya*-like hormogonia that are marked with an Asterix. (D) CLSM image showing the *Nostoc*-like stage. (E) germination of akinetes. (F) *Chlorogloeopsis*-like stage. (G) *Chlorogloeopsis*-like stage with brownish akinetes. (H) *Pseudanabaena*/*Leptolyngbya*-like motile hormogonia. [Color figure can be viewed at [wileyonlinelibrary.com](http://wileyonlinelibrary.com)]



TABLE 1. Morphological comparison of *Cyanocohniella* species.

			<i>Cyanocohniella calida</i>	<i>Cyanocohniella crotaloides</i> sp. nov.
Color			Blue-green	Blue-green
Filaments			Hypervariable, mainly <i>Nostoc</i> -like, rarely with heterocytes	Hypervariable, mainly <i>Nostoc</i> -like, rarely with heterocytes
Hormogonia			<i>Pseudanabaena</i> / <i>Leptolyngbya</i> -like, motile	<i>Pseudanabaena</i> / <i>Leptolyngbya</i> -like, motile
Akinetes			Single or in series, spherical to oval, often with yellowish cell walls, 4–8(10) µm in diameter	Single or in series attached to <i>Chlorogloeopsis</i> -like filaments, spherical to oval, often yellowish, 2.8–6.3 µm in diameter
Necridia			Absent	Absent
Development:	Young filaments	Cell form	<i>Pseudanabaena</i> / <i>Leptolyngbya</i> -like, cylindrical, (1) 1.5(2) µm wide, with intercalary cells (1) 1.5–2.5 µm long	<i>Pseudanabaena</i> / <i>Leptolyngbya</i> -like, cylindrical, 1.5–3.1 µm wide
		Constriction	None or slightly at cross walls	Marked
		Sheath	None or fine, colorless to yellowish	None or fine, colorless
		Apical cells	Longer than wide 1.5–2.5 µm, oval to conical, no calyptra	Longer than wide 1.5–3.1 µm, oval to slightly conical, no calyptra
	Adult filaments	Cell form	<i>Nostoc</i> -like, oval to spherical (2) 3.0–4.5(5) µm in diameter, intercalary oval to spherical heterocytes 5–6(7) µm, one- to two-celled apical hormocytes	<i>Nostoc</i> -like, round to spherical 2.1–3.7 µm in diameter,
		Constriction	Marked, attenuated toward apices	Marked
		Sheath	Unlamellated, slightly attenuated toward apices	None or fine, colorless
		Apical cells	Similar in form to common cells	Similar in form to common cells
	Mature filaments	Cell form	<i>Chlorogloeopsis</i> -like, cells spherical, oval, or irregularly shaped, 2–7(8) µm in diameter, with cells irregularly arranged in ensheathed filaments, sometimes evidencing cell division in two planes, partly biserial, with heterocytes rarely present, one- to two-celled apical hormocytes	<i>Chlorogloeopsis</i> -like, cells spherical, oval, or irregularly shaped, 2.6–5 µm in diameter, with cells irregularly arranged in ensheathed filaments, sometimes evidencing cell division in two planes, partly biserial, with heterocytes rarely present, apical, and intercalary hormocytes
		Sheath	Colorless to slightly yellow, usually thin, unlamellated	Colorless, usually thin, unlamellated
		Apical cells	Similar in form to common cells	similar in form to common cells
Habitat			Thermal water (47°C), Karlovy Vary, Czech Republic	Beach mat, Schiermonnikoog, Netherlands

in the secondary structures (Fig. 3) with three helices that are quite similar, especially D-D1' and Box B. Main differences are in the loops, but there are also several in paired regions (D1-D1' and V3). The V3 helix is shorter than in *C. calida*.

**Differentiation against other species:** The newly isolated strain *Cyanocohniella crotaloides* PJ S45 has smaller cells than *Cyanocohniella calida* during almost all life stages. Also, the apical cells of the *Leptolyngbya*/*Pseudanabaena*-like stage are only slightly conical in contrast to the conical tips of *C. calida*. Akinetes mainly stay attached in uni- to multiseriate strings to the *Chlorogloeopsis*-like filaments and are only rarely found singularly, whereas those of *C. calida* are detached from the main filaments as cell rows or single units. It can also be separated from *Komarekiella atlantica* because the latter forms rounded macrocolonies, abundant heterocytes, and quadratic cells during the hormogonium stage.

***Oculatella crustae-formantes*, P. Jung, Briegel-Williams, Mikhailyuk et Büdel sp. nov. (Fig. 4, Table 2).**

**Description:** The species has single filaments without false branching that are 0.8–1.6 µm wide with a firm sheath. The trichomes and single cells are 0.5–1.1 µm wide (0.7 µm in average)/1.2–2.9 µm long, frequently granulated, and constricted at the cross walls with a parietal organization of the thylakoids. Apical cells are longer than broad, 0.6–2.5 µm wide/1.5–7.7(9.5) µm long with the typical orange 'eye-spot' in the very tip of the apical cells of mature filaments. The species tested positively for nodularin/microcystin genes.

**Habitat:** Biological soil crusts

**Etymology:** '*crustae-formantes*' after the presence of the species among a cyanobacterial-dominated biological soil crust

**Type locality:** -NORWAY. Arctic, Spitsbergen, Geopol, elev. 64 m, 78°56'58.38" N, 11°28'35.64" E,

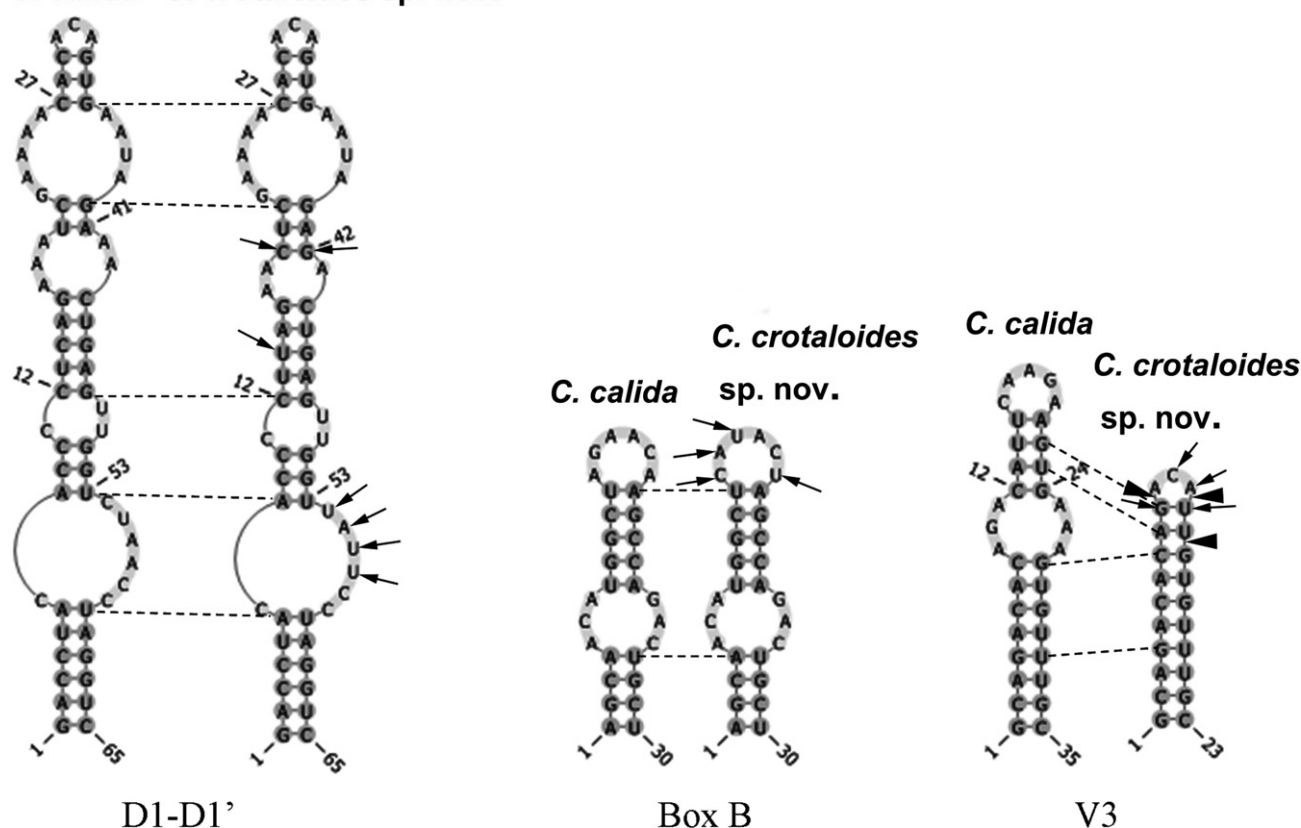
***C. calida* *C. crotaloides* sp. nov.**

FIG. 3. Secondary structure of the main informative helices of region 16S–23S ITS of *Cyanocohniella* species. All differences between strains are presented in comparison to the authentic strain of *C. calida* (CCALA 1049). Variable bases are shown with arrows, places of insertions/deletions of base pairs are marked with arrowheads, homologous base pairs among both species are indicated by dotted lines.

collected by L. Briegel-Williams in 2015, and isolated by P. Jung.

**Holotype:** The preserved holotype specimen is available via Herbarium Hamburgense, Hamburg, Germany (HBG024671). It was prepared from the living strain which was the source of 16S, ITS, and 23S rRNA gene sequence deposited as GenBank accession number MN243147.

**Reference strain:** The reference strain is available via the culture collection DSMZ Braunschweig (DSM 109267) and the culture collection SAG of Göttingen, Germany (SAG 2593).

**Phylogenetic relations and secondary structure of the 16S–23S ITS:** A total of 111 sequences of representative taxa were included in the phylogenetic analyses to assess the placement of the *Oculatella* clade in the cyanobacteria (Fig. 4A). The ML and Bayesian inference analyses produced similar tree topologies in our phylogenies. *Oculatella crustae-formantes* sp. nov. falls within the *Oculatella* clade (95.6%–98.8%) at a separated position (Fig. 4A, Table S3 in the Supporting Information). Additionally, dissimilarity of >16.2% could be detected among the 16S–23S ITS genes of all tested *Oculatella* species (Table S4 in the Supporting Information). Secondary structures of main informative helices of

16S–23S ITS showed general similarity with known species, but also some variability (Fig. 5): multiple differences in paired regions and loops of D1–D1', Box B, and V2 helices. The V3 helix is longer than in known species and characterized by multiple insertions of base pairs in the middle part.

**Differentiation against other species:** *Oculatella crustae-formantes* sp. nov. differs by having smaller minimum widths (0.7 µm in average) than all other known species (minimum widths varying from 0.8 to 1.6 µm) and never shows false branching or multiple filaments in one sheath.

*Aliterella chasmolithica*, P. Jung, Schermer, Mikhailuk et Büdel sp. nov. (Fig. 6, Table 3).

**Description:** Microscopic irregular or rounded colonies with variable number of cells (up to 32–64 cells or more), usually aggregated into irregular, extended, compact multicolonial groups, sometimes solitary cells. Mucilage unstratified, colorless, and firm surrounding cells and colonies. Cells mostly irregular to rounded, 1.5–3.2 µm long, 1.5–2.4 µm in diameter with parietal thylakoids. Cell contents blue-green, slightly granulated, or sometimes homogeneous. Thylakoids parietal. Reproduction by simple binary cell division in three or more planes. The

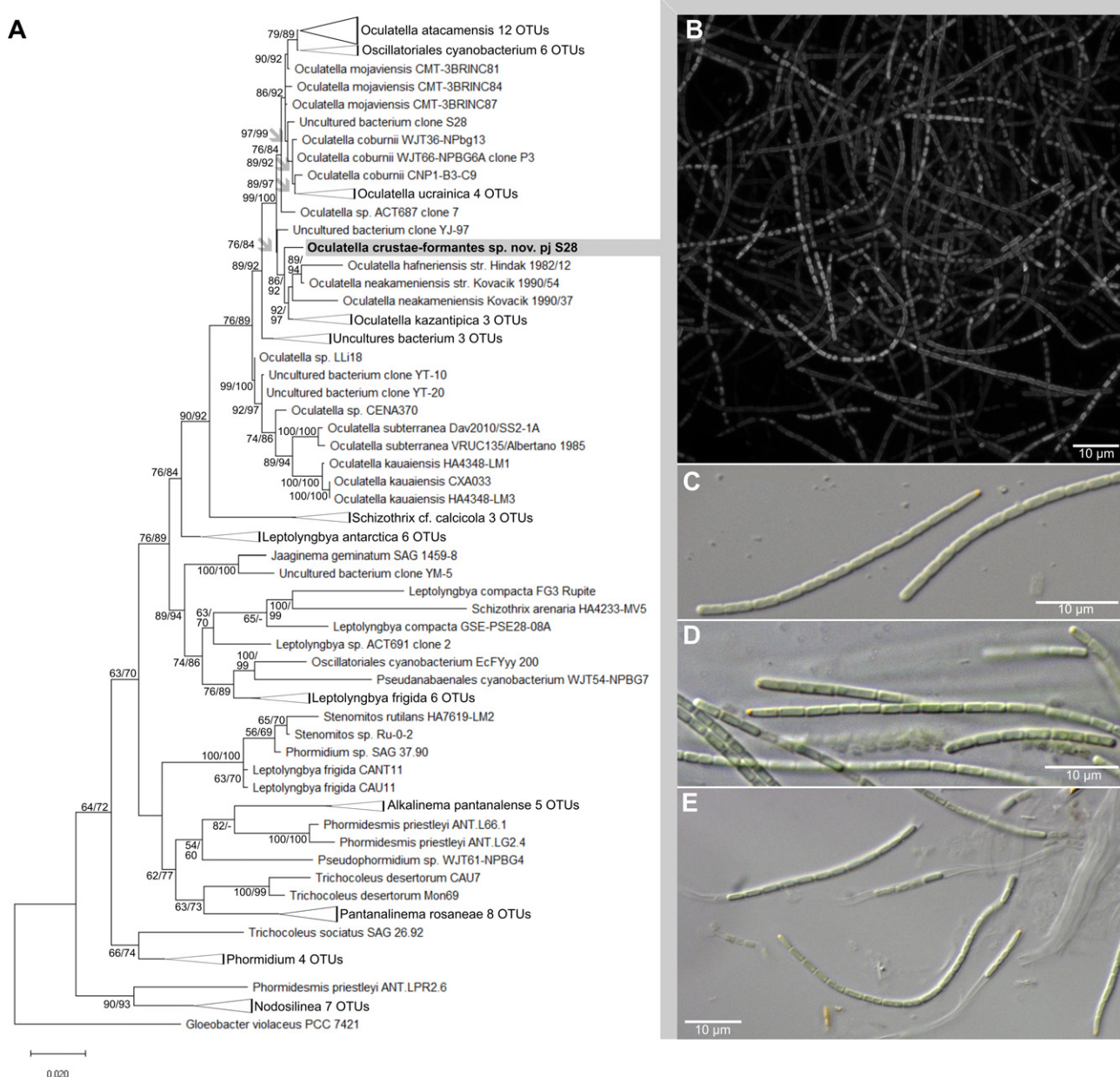


FIG. 4. Phylogenetic tree and micrographs of *Oculatella crustae-formantes* sp. nov. (A) phylogenetic position of *Oculatella crustae-formantes* sp. nov. based on the 16S rRNA gene sequence data rooted to *Gloeobacter violaceus* PCC 7421. Numbers at nodes represent first the ML bootstrap support (values  $\geq 50\%$ ) and second the posterior probabilities from the Bayesian analysis (values  $\geq 50\%$ ). The scale indicates the numbers of substitutions per site. (B) CLSM image, (C–E) filaments with sheaths and yellow 'eye-spot' at the tip of mature filaments. [Color figure can be viewed at [wileyonlinelibrary.com](http://wileyonlinelibrary.com)]

species tested negatively for nodularin/microcystin genes.

**Habitat:** Chasmothitic in boulders of granite.

**Etymology:** 'chasmothitica' after the chasmothitic occurrence of the species within fissures and cracks of granite stones and rocks.

**Type locality:** -CHILE. Atacama Desert: Pan de Azúcar National Park, elev. 409 m, 26°06'39.62" S; 70°32'54.51" W, collected on July 23, 2017, and isolated by P. Jung.

**Holotype:** The preserved holotype specimen is available via Herbarium Hamburgense, Hamburg, Germany (HBG024669). This was prepared from the living strain which was the source of 16S, ITS, and 23S rRNA gene sequence deposited as GenBank accession number MN243145.

**Reference strain:** The reference strain is available via the culture collection DSMZ Braunschweig (DSM 109265) and the culture collection SAG of



TABLE 2. Morphological comparison of *Oculatella* species.

	<i>O. atacamensis</i>	<i>O. coburnii</i>	<i>O. mojaviensis</i>	<i>O. neokamienensis</i>	<i>O. kazantipica</i>	<i>O. ucrainica</i>	<i>O. cataractarum</i>	<i>O. hafneriensis</i>	<i>O. kauaiensis</i>	<i>O. subharricana</i>	<i>O. crustae-formantes</i> sp. nov.
Filament width, $\mu\text{m}$	1.8–4.1	1.7–2.8	2.0–2.6	1.2–4.1	(1.3) 1.5–5 –7.5	(1.5) 2.5– (3.0)	1.3–1.7	1.4–2.4	1.2–1.7	1–2	0.8–1.6
Sheath	Common	Common	Common	Common	Common	Common	Rare	Common	Common	Common	Common
False branching	Rare	Rare	Rare	Absent	Rare	Rare	Rare	Absent	Absent	Rare	Absent
Trichome/cell	1.5–2.3	1.4–4.8	1.6–2.2	1.2–1.7	1.1–1.3– 1.7	(1.3)–1.7– 2.5	0.8–1.3– (1.7)	1.1–1.9	0.9–1.4	ND	0.5–1.1
width, $\mu\text{m}$											
Constrictions	Weak	Absent/ weak	Absent/ weak	Absent/weak	Absent/ weak	Clear	Absent/ weak	Absent/weak	Absent/weak	Abundant	Abundant
Granulation at cross walls	Sometimes	Absent	Sometimes	Sometimes	Sometimes	Sometimes	Frequently	Sometimes	Absent	Absent	Frequently
Necridia											
Cell length, $\mu\text{m}$	–	–	+	–	–	–	–	–	–	–	–
Apical cells, width/length, $\mu\text{m}$	1.5–7.4 1.4–2.1/2.5–9.9	1.8–4.8 1.4–1.8/ 2.4–5.4	1.5–5.0 1.4–2.0/ 2.4–6.8	1.5–5.4 1.1–1.7/2.3–7.7	(2)2.3–4.7 (7.5) 1.3–1.5/ (4)5–7 (8.7)	(1.3)1.7– 3.7(4.7) 1.3–1.7 (2.3)/ (2.3)3.3– 6.7(7.7)	(1.4)–1.6– 6.8–(8.7) /2.1–7.7– (12.8)	1.0–4.4 1.0–1.7/2.0– 5.8	1.0–4.4 0.9–1.5/1.3– 7.8	1.5–3 ND	1.2–2.9 0.6–2.5/1.5– 7.7(9.5)
Habitat	Soils and under quartz rocks, Atacama Desert	Ganitic soil in hot desert, Mojave Desert, USA	Dolomitic soil, Mojave Desert, USA	Semi-arid volcanic soil, Nea Kameni Island, Greece	Conquina beach, Ukraine	Chalk outcrops, Conquina beach, Ukraine	Dripping sandstone rocks, Calif creek falls, USA	Lake benthos Hafnersee, Austria	Sea cave Island of Kauai, USA	Hypogaea, Catacombs, Rome, Italy	Soils,

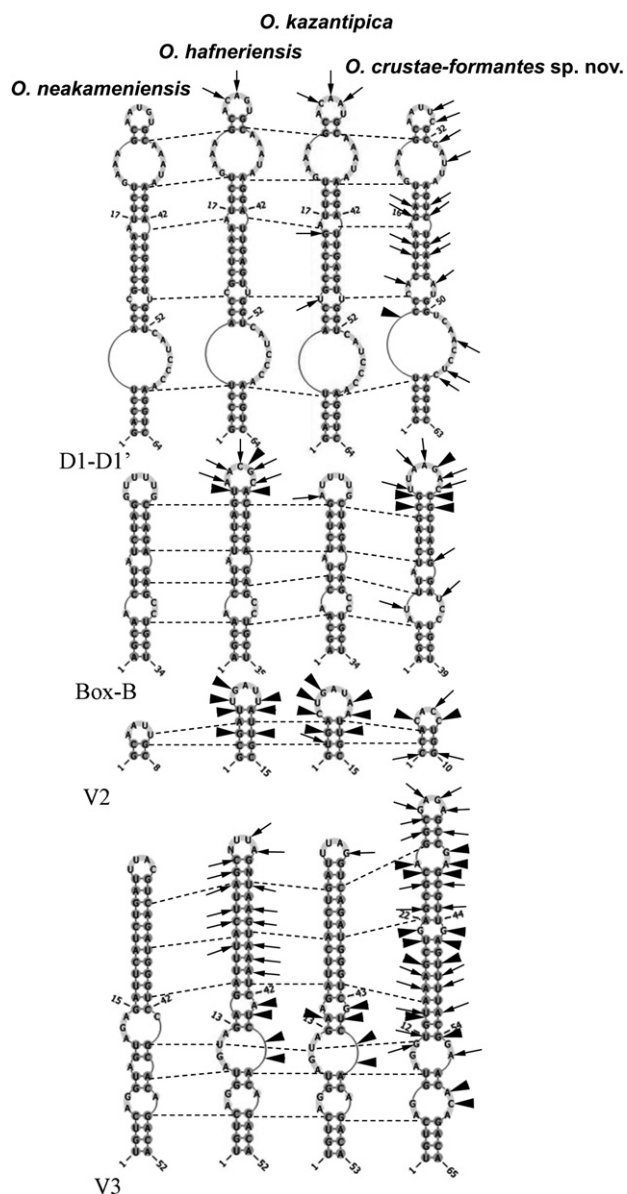


FIG. 5. Secondary structure of the main informative helices of region 16S–23S ITS of some terrestrial *Oculatella* species. All differences between strains are presented in comparison to the authentic strain of *O. neakamienensis* (Kovacic 1990/54). Variable bases are shown with arrows, places of insertions/deletions of base pairs are marked with arrowheads, homologous base pairs among different species are indicated by dotted lines.

Göttingen, Germany (temporary strain number SAG NA2019.003).

**Phylogenetic relations and secondary structure of the 16S–23S ITS:** A total of 54 sequences of representative taxa were included in the phylogenetic analyses to assess the placement of the *Aliterella* clade in the Cyanobacteria (Fig. 6A). The ML and Bayesian inference analyses produced similar tree topologies in our phylogenies. *A. chasmolithica* sp. nov. joins a clade of uncultured bacterial OTUs (97.6–98.8% similarity) in close vicinity to the three

known *Aliterella* species: *A. atlantica* (93.7%), *A. antarctica* (96.5%) and *A. shaanxiensis* (97.2%; Fig. 6A, Table S5 in the Supporting Information). Furthermore, dissimilation of >12.8 % could be observed within the 16S–23S ITS genes of *Aliterella* strains during p-distance calculations (Table S6 in the Supporting Information). The secondary structure of the main informative helices of 16S–23S ITS (Fig. 7) shows some differences in paired regions and loops of the upper part of D1–D1' helix as well as lower and upper part of Box B helix.

**Differentiation against other species:** The described species *Aliterella chasmolithica* can be distinguished from *A. atlantica*, *A. antarctica*, and *A. shaanxiensis* by a smaller cell size. It can further be distinguished from *A. shaanxiensis* by more rounded cells.

## DISCUSSION

According to the polyphasic approach, the concept of cyanobacterial genera and especially species descriptions should comprise a unique phylogenetic position, distinct morphological separation, as well as related ecological factors (Komárek et al. 2014). Nowadays, genera are rather unambiguously defined as a collection of species that forms a monophyletic clade (e.g., González-Resendiz et al. 2019). However, the discussion about ‘what constitutes a species?’ based on genetics started even before Stackebrandt and Goebel (1994) suggested that strains with <97.5% 16S rRNA sequence similarity should be considered as separate species, while those with less than 95% similarity should likely be considered as separate genera.

Stackebrandt (2006) changed the cut-off points to higher values which was even more strictly supported by the cut-offs proposed in Yarza et al. (2014; 98.7% for species, 94.5% for genera). Many recent studies have shown that cyanobacterial species have distinct morphological features even above a similarity level of 97.5% (Osorio-Santos et al. 2014, González-Resendiz et al., 2019, Konstantinou et al. 2019) and some authors even suggest a cut-off level for, for example, genera within the *Nostocales* of 98% similarity and for species of <99% (Kaštovský et al. 2014). An additional and recent example for comparable cut-off levels in pleurocapsalean cyanobacterium *Odorella benthonica* that shows 99.92% similarity to *Pleurocapsa minor* JQ070059 and is separated by striking morphological and ecological differences (Shalygin et al. 2019). For these reasons the p-distance dissimilarity analysis of the ITS appears as a valuable addition to the molecular setup that has been applied since a few years at least for cryptic taxa (e.g., González-Resendiz et al. 2019). Nevertheless, similarity cut-off levels always represent only a part of the evidence to separate genera or species.

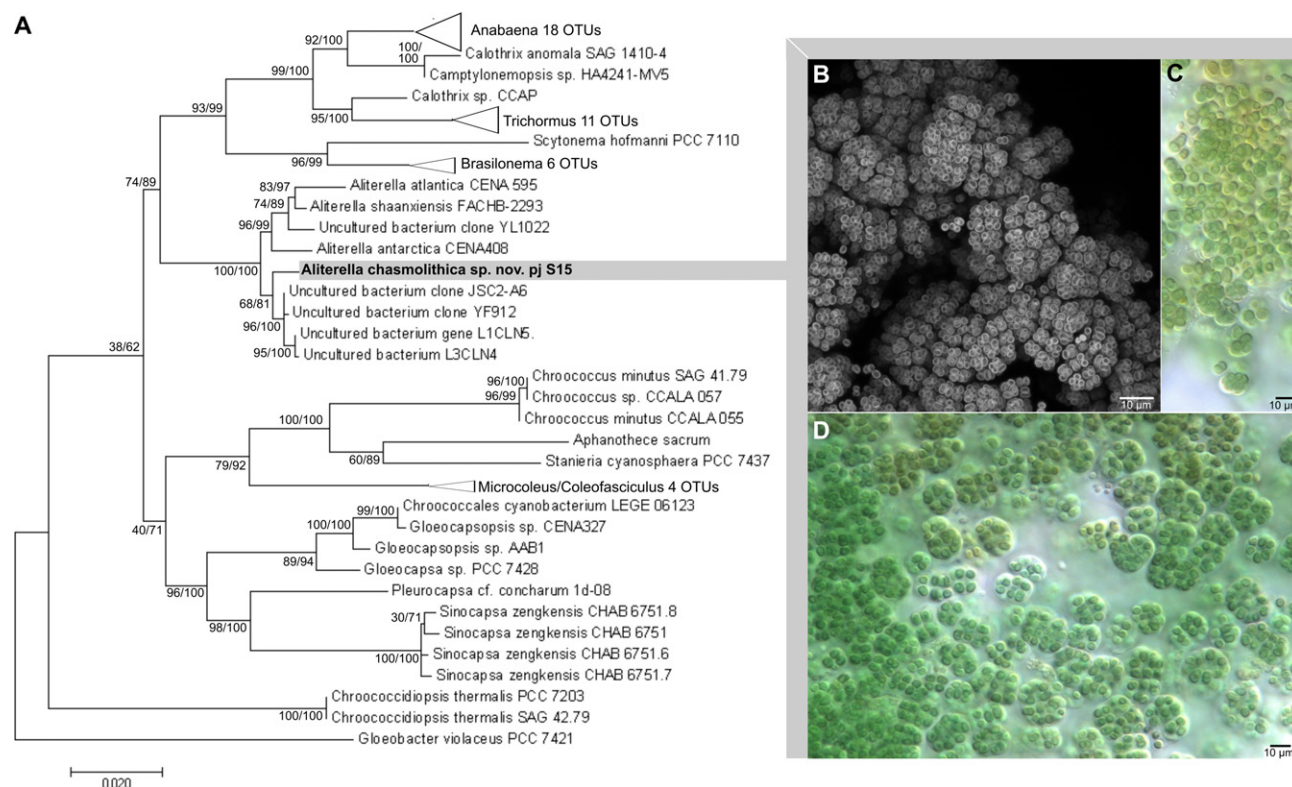


Fig. 6. Phylogenetic tree and micrographs of *Aliterella chasmolithica* sp. nov. (A) Phylogenetic position of *Aliterella chasmolithica* sp. nov. based on the 16S rRNA gene sequence data rooted to *Gloeobacter violaceus* PCC 7421. Numbers at nodes represent first the ML bootstrap support (values  $\geq 50\%$ ) and second the posterior probabilities from the Bayesian analysis (values  $\geq 50\%$ ). The scale indicates the numbers of substitutions per site. (B) CLSM image of *Aliterella* sp. nov. (C) and (D) compact and irregular thallus composed of numerous colonies or solitary cells with colorless and firm mucilaginous envelope. [Color figure can be viewed at [wileyonlinelibrary.com](http://wileyonlinelibrary.com)]

The assignment of such a new species or genus to a specific ecological niche or substrate can be seen as an extension of the polyphasic approach, but it will remain not more than a careful assumption in most cases. Nevertheless, the idea of a distinct habitat or substrate specificity developed from well-known cases of a number of genera can clearly show restrictions to marine, thermic, or even terrestrial locations. For example, some freshwater aquatic genera such as *Dolichospermum*, *Aphanizomenon*, *Cylindrospermopsis*, and *Woronichinia* were not found outside the freshwater habitat niche. There is also a series of species such as the subaeric *Komarekiella atlantica* that are restricted to the tropics (Hentschke et al. 2017). This might be linked to their inability to survive freezing (Neustupa and Škaloud 2008) or to the knowledge that other strains prefer or even exclusively occur under arid conditions such as *Gloeocapsopsis* sp. AAB1 (Azua-Bustos et al. 2014) or *Spirirestris rafaensis* (Flechtner et al. 2002). This is still challenging even for already established genera and species and should be stated carefully because the inventory of cyanobacterial species is by far not complete as this study demonstrates. Especially genera that comprise only one or a few species with a putative ecology could hold

some surprises because future studies will easily be able to add further species to a genus that might be from opposing habitats.

Cyanocohniella. Kaštovský et al. (2014), for example, already considered an unresolved ecology of the genus *Cyanocohniella* by pointing out that *C. calida* might be found all over the world, analog to *Mastigocladus laminosus* (Petersen 1923, Miller et al. 2007, Finsinger et al. 2008), since both species are sharing the same type of habitat, namely, thermal springs. Our finding of *C. crotaloides* sp. nov. as a highly related species from the North Sea demonstrates that the genus does not seem to be a purely thermophilic clade. However, a certain thermotolerance would probably still be given also in *C. crotaloides* sp. nov. because it appears in algal beach mats which are regularly exposed to the sun. Quartz sand in combination with reflections from water puddles could easily reach temperatures beyond  $50^{\circ}\text{C}$  at least during the summer months. It remains speculative whether this assumed thermotolerance gives *C. crotaloides* sp. nov. a competitive advantage over other taxa within microbial mats described as highly diverse (Bauersachs et al. 2011). Testing this hypothesis might be challenging since *C. crotaloides* sp. nov. is very unstable in its morphology, with a

TABLE 3. Morphological comparison of *Aliterella* species.

	<i>A. atlantica</i>	<i>A. antarctica</i>	<i>A. shaanxiensis</i>	<i>A. chasmolithica</i> sp. nov.
Thallus	Extended, compact, irregularly shaped, composed of numerous colonies or isolated ensheathed cells	Extended, compact, irregularly shaped, composed of numerous colonies or isolated ensheathed cells	Extended, compact, irregularly shaped, composed of numerous colonies or isolated ensheathed cells	Extended, compact, irregularly shaped, composed of numerous colonies or rarely isolated ensheathed cells
Colony shape	Mostly irregular, sometimes rounded	Mostly irregular, sometimes rounded	Mostly irregular, sometimes rounded	Mostly irregular, sometimes rounded
Number of cells in colony	Variable (up to 32–64 cells or more)	Variable (up to 32–64 cells or more)	Variable (up to 32–64 cells or more)	Variable (up to 32–64 cells or more)
Mucilage	Firm surrounding cells and colonies, colorless	Firm surrounding the cells and colonies, colorless to brownish	Firm surrounding cells and colonies, colorless	Firm surrounding the cells and colonies, colorless to brownish
Cell size	3.0–4.8 $\mu\text{m}$ long (mean = 3.7 $\mu\text{m}$ ), 2.0–3.3 $\mu\text{m}$ diameter (mean = 2.7 $\mu\text{m}$ )	3.4–5.8 $\mu\text{m}$ long (mean = 4.5 $\mu\text{m}$ ), 2.5–4.6 $\mu\text{m}$ in diameter (mean = 3.5 $\mu\text{m}$ )	2.8–3.7 $\mu\text{m}$ long (mean = $3.3 \pm 0.3$ $\mu\text{m}$ , $n = 40$ ), 2.0–2.7 $\mu\text{m}$ in diameter (mean = $2.2 \pm 0.2$ $\mu\text{m}$ , $n = 40$ )	1.5–3.2 $\mu\text{m}$ long (mean = $2.6 \pm 0.4$ ), 1.5–2.4 $\mu\text{m}$ in diameter (mean = $1.9 \pm 0.2$ )
Length/Diameter	1.1–2 (mean = 1.4)	1.0–1.7 (mean = 1.3)	1.3–1.7 (mean = 1.5)	0.7–2.0 (mean = $1.3 \pm 0.2$ )
Cell shape	Cylindrical with rounded ends, sometimes irregular	Cylindrical with rounded ends or, less frequently, near spherical, or irregular	Cylindrical with rounded ends	Cylindrical with rounded ends or, less frequently, near spherical, or irregular
Cell content	Granulated, sometimes homogeneous	Granulated, sometimes homogeneous	Slightly granulated, sometimes homogeneous	Granulated, sometimes homogeneous
Color	Blue-green	Blue-green	Blue-green	Blue-green
Thylakoids	Irregular with a higher concentration in the cell periphery	Irregular with a higher concentration in the cell periphery	Parietal	Parietal
Reproduction	Simple binary cell division in three or more planes	Simple binary cell division in three or more planes	Simple binary cell division in three or more planes	Simple binary cell division in three or more planes
Habitat	Marine planktonic, Atlantic Ocean	On polar coastal ornithogenic soil, Antarctica	Freshwater planktonic, China	Chasmoendolithic in granite, Atacama Desert

life cycle (Fig. 2, B–H) that is among the most complex ones observed in all of the cyanobacteria which makes the taxon difficult to identify especially in environmental samples. The various stages of both *Cyanocohniella* species can easily be mixed up with *Pseudanabaena*, *Nostoc*, and *Chlorogloeopsis* species. In contrast, *Cyanocohniella crotaloides* sp. nov. can easily be distinguished from *C. calida* by its multiseriate brownish akinetes that remain attached to the *Chlorogloeopsis*-like filament and contribute to the rattle-like appearance (Fig. 2B). The morphologically similar cyanobacterium *Komarekiella atlantica* was described in 2017 by Hentschke et al. It grew on the bark of trees, wood, and concrete in the Brazilian Atlantic rainforest and Hawaii and shares the complex life cycle. This species differs from *C. calida* and *C. crotaloides* by its rounded macrocolonies, abundant heterocytes, and the quadratic cells during the hormogonium stage. Interestingly, *K. atlantica* is phylogenetically more related to *Goleter* and *Roholtiella* than to *Cyanocohniella* (Fig. 2), although the two genera are morphologically alike. In contrast, both *Cyanocohniella* species are rather closely related (Table S1; 99.9%) with only one nucleotide

difference in the 16S rRNA and large dissimilarities within the 16S–23S ITS regions as demonstrated by p-distance calculations (Table S2; 12.7%). Furthermore, the secondary structures (Fig. 3) such as several different bases in the paired region of the D1–D1' and V3 helices as well as a shorter V3 helix in comparison to *C. calida* support the definition of *C. crotaloides* sp. nov. as a new species within the genus.

**Oculatella.** Since its separation from the Lep-  
tolyngbyaceae in 2012 by Zammit et al. (2012) until today, 11 species have been described belonging to the genus *Oculatella*. Although the morphological characteristics, which allow a differentiation between the species, are rather cryptic, the 16S rRNA enables further distinction (e.g., Osorio-Santos et al. 2014). The single *Oculatella* species is worth taxonomic recognition and a further split, as it allows insights into its pattern of speciation, a rare exception regarding investigations of the biogeography within one cyanobacterial genus. The genus comprises very rare if not endemic species such as *O. atacamensis*, *O. kauaiensis*, *O. cataractarum*, and *O. hafneriensis* (Osorio-Santos et al. 2014), besides others that are

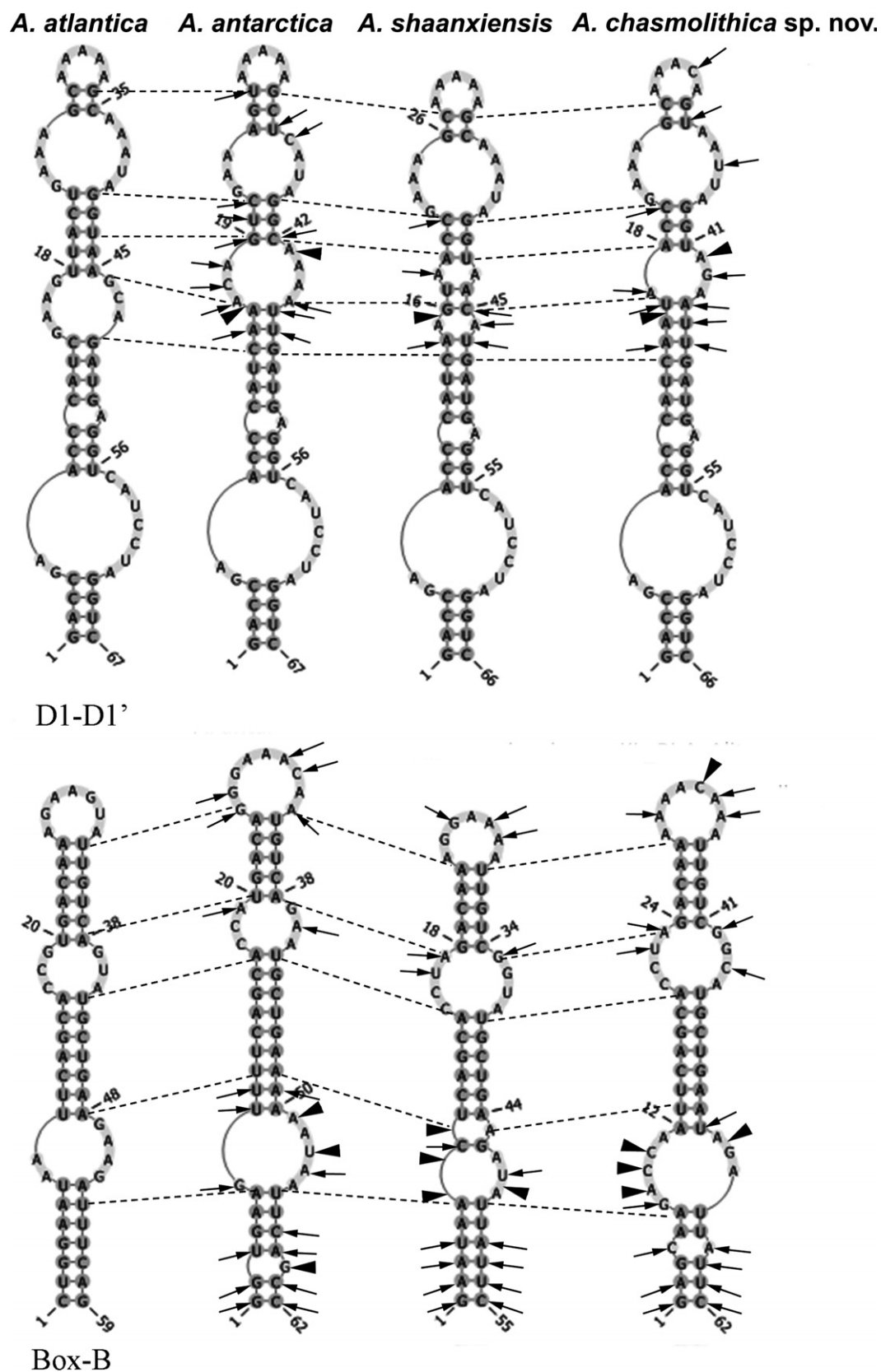


FIG. 7. Secondary structure of the main informative helices of region 16S–23S ITS of *Aliterella* species. All differences between strains are presented in comparison to the authentic strain of *A. atlantica* (CENA 595). Variable bases are shown with arrows, places of insertions/deletions of base pairs are marked with arrowheads, homologous base pairs among different species are indicated by dotted lines.



more frequently occurring with a broader geographical extension such as *O. subterranea* (Komárek and Anagnostidis 2005, Zammit et al. 2012). However, the newly described *O. crustae-formantes* sp. nov. is the first report of an *Oculatella* species from a considerable cold habitat in the high Arctic. This demonstrates that the movement of propagules of *Oculatella* species across great distances (via e.g., water, wind, migratory birds), which subsequently leads to speciation seems to be not as rare as speculated by Osorio-Santos et al. (2014). Besides its remote origin and ecology, *O. crustae-formantes* sp. nov. can be separated from all other species within the genus by its small cell size with filament widths that rarely exceed 1.6 µm (Fig. 4, B–E; Table 2). Phylogenetically it forms a separate lineage in *Oculatella*, with highest similarity of 16S rRNA to *O. ucrainica* (Table S3, 98.8%). Separation of this strain is also supported by high dissimilarity values of the 16S–23S ITS gene region (Table S4). P-distance analysis also indicates that the initial species concept within the genus *Oculatella* might be too narrow since the dissimilarity percentage among *O. kazantipica*, *O. ucrainica*, *O. atacemensis*, *O. coburnii*, and *O. neakameniensis* are below the threshold of 3%. The secondary structure of informative helices of 16S–23S ITS (Fig. 5) shows differences in paired regions and loops of D1–D1', Box-B, and V2 helices and multiple insertions of base pairs in the middle part of V3 helix.

*Aliterella*. The presence of an *Aliterella* species within naturally occurring cracks and fissures of granite boulders from the Atacama Desert clearly points to the fact that the genus is not strictly aquatic. During the phylogenetic analysis, *A. chasmolithica* sp. nov. showed highest similarities to the uncultured bacterium YF912 (Table S5; 89.8%) which was isolated from a natural carbonate surface in the Yunnan stone forest of China. Our strain clusters together with the latter and a few other uncultured bacterial strains in distance to the described species *A. shannxiensis*, *A. antarctica*, and *A. atlantica* which could indicate a split in the genus between aquatic and terrestrial/lithophilous species. Rigonato et al. (2016) as well as Zhang et al. (2018) already stated that it is likely that the genus could have a broad ecological amplitude which might be clarified during future discoveries of further species that belong to this genus. However, both author teams proposed the new monotypic family *Aliterellaceae* within the order *Chroococcidiopsidales* to accommodate this genus, which is supported by our data. This can be compared to the novel and highly related *Sinocapsaceae* which was suggested incertae sedis recently, with *Sinocapsa zengkensis* CHAB 6571 (*Aliterella antarctica* CENA 408 had the maximum similarity with 94%; Fig. 6) as the only member since the order *Chroococcidiopsidales* is currently not monophyletic (Wang et al. 2019). Besides its ecology, *A. chasmolithica* sp. nov. also differs from the three described

species mainly by a smaller cell size (Fig. 6, B–D; Table 3). The secondary structure of the main informative helices of 16S–23S ITS (Fig. 7) shows some differences in paired regions and loops of D1–D1' and Box B helices.

## CONCLUSIONS

The three new cyanobacterial species *Cyanocohniella crotaloides* (Schiermonnikoog Island, Netherlands), *Oculatella crustae-formantes* (Spitsbergen, Arctic), and *Aliterella chasmolithica* (Atacama Desert, Chile) described here contribute to the overall understanding of the three recently established genera and are broadening the ecological amplitude of each of them. The new species allow new insights into the identities of several uncultured cyanobacterial sequences available in the GenBank database, which are likely belonging to these three genera. We would like to encourage future descriptions of even cryptic taxa that lack well-developed morphological characteristics by comparing also the p-distance dissimilarity as a holistic approach since this helps to aim for a more complete species inventory and to understand the ecology as well as the biogeography of cyanobacterial genera.

## ACKNOWLEDGMENTS

The authors would like to thank Michelle Gehringer for support during the toxin screening and Arianna Gallo for her help during the phylogenetic analysis and Wolf-Rüdiger Arendholz for support with the Latin names of the new species. We also would like to thank Anne Thyssen for her support during the CLSM analyses. PJ, BB, and KB have been supported by the German Research Foundation (projects BU 666/17, 18, 19; LE 903/14). TM thanks Alexander von Humboldt Foundation (Germany) for financial support.

- Albertano, P., Barsanti, L., Passarelli, V. & Gualtieri, P. 2000. A complex photoreceptive structure in the cyanobacterium *Lepolyngbya* sp. *Micron* 31:27–34.
- Albertano, P. & Grilli Caiola, M. 1988. Structural and ultrastructural characters of a red biodeteriorating *Lyngbya* sp. in culture. *Arch. Hydrobiol. Supplement Volumes*: 55–57.
- Azua-Bustos, A., Zúñiga, J., Arenas-Fajardo, C., Orellana, M., Salas, L. & Rafael, V. 2014. *Gloeocapsopsis* AAB1, an extremely desiccation-tolerant cyanobacterium isolated from the Atacama Desert. *Extremophiles* 18:61–74.
- Bauersachs, T., Compaoré, J., Severin, I., Hopmans, E. C., Schouten, S., Stal, L. J. & Sinninghe Damsté, J. S. 2011. Diazotrophic microbial community of coastal microbial mats of the southern North Sea. *Geobiol.* 9:349–59.
- Baumann, K., Jung, P., Samolov, E., Lehnert, L. W., Büdel, B., Karsten, U., Bendix, J. et al. 2018. Biological soil crusts along a climatic gradient in Chile: richness and imprints of phototrophic microorganisms in phosphorus biogeochemical cycling. *Soil Biol. Biochem.* 127:286–300.
- Bischof, H. & Bold, H. 1963. *Some Soil Algae From Enchanted Rock and Related Algal Species*. University of Texas Publications, Austin, TX, USA. 6318:1–95.
- Byun, Y. & Han, K. 2009. PseudoViewer3: generating planar drawings of large-scale RNA structures with pseudoknots. *Bioinformatics* 25:1435–7.

- Engene, N., Cameron Coates, R. & Gerwick, W. H. 2010. 16S rRNA gene heterogeneity in the filamentous marine cyanobacterial genus *Lyngbya*. *J. Phycol.* 46:591–601.
- Erwin, P. M. & Thacker, R. W. 2008. Cryptic diversity of the symbiotic cyanobacterium *Synechococcus spongiarum* among sponge hosts. *Mol. Ecol.* 17:2937–47.
- Finsinger, K., Scholz, I., Serrano, A., Morales, S., Uribe-Lorio, L., Mora, M., Sittenfeld, A., Weckesser, J. & Hess, W. R. 2008. Characterization of true-branching cyanobacteria from geothermal sites and hot springs of Costa Rica. *Env. Mic.* 10:460–73.
- Flechtner, V. R., Boyer, S. L., Johansen, J. R. & DeNoble, M. L. 2002. *Spirirestis rafaellensis* gen. et sp. nov. (Cyanophyceae), a new cyanobacterial genus from arid soils. *Nova Hedwigia* 74:1–24.
- Gehring, M. M., Adler, L., Roberts, A. A., Moffitt, M. C., Mihali, T. K., Mills, T. J., Fieker, C. & Neilan, B. A. 2012. Nodularin, a cyanobacterial toxin, is synthesized in planta by symbiotic *Nostoc* sp. *ISME J.* 6:1834.
- González-Resendiz, L., Johansen, J. R., León-Tejera, H., Sánchez, L., Segal-Kischinevsky, C., Escobar-Sánchez, V. & Morales, M. 2019. A bridge too far in naming species: a total evidence approach does not support recognition of four species in *Desertifilum* (Cyanobacteria). *J. Phycol.* 55:898–911.
- Hentschke, G. S., Johansen, J. R., Pietrasiak, N., Rigonato, J., Fiore, M. F. & Santanna, C. L. 2017. *Komarekiella atlantica* gen. et sp. nov. (Nostocaceae, Cyanobacteria): a new sub-aerial taxon from the Atlantic Rainforest and Kauai, Hawaii. *Fottea* 17:178–90.
- Johansen, J. R. & Casamatta, D. A. (2005). Recognizing cyanobacterial diversity through adoption of a new species paradigm. *Algal studies* 117:71–93.
- Jung, P., Briegel-Williams, L., Schermer, M. & Büdel, B. 2019a. Strong in combination: polyphasic approach enhances arguments for cold-assigned cyanobacterial endemism. *MicrobiologyOpen* 8:e00729.
- Jung, P., Schermer, M., Briegel-Williams, L., Baumann, K., Leinweber, P., Karsten, U., Lehnert, L., Achilles, S., Bendix, J. & Büdel, B. 2019b. Water availability shapes edaphic and lithic cyanobacterial communities in the Atacama Desert. *J. Phycol.* 55:1306–18.
- Jungblut, A. D. & Neilan, B. A. 2006. Molecular identification and evolution of the cyclic peptide hepatotoxins, microcystin and nodularin, synthetase genes in three orders of cyanobacteria. *Arch. Microbiol.* 185:107–14.
- Kaštovský, J., Gomez, E. B., Hladil, J. & Johansen, J. R. 2014. *Cyanocohmiella calida* gen. et sp. nov. (Cyanobacteria: Aphani-zomenonaceae) a new cyanobacterium from the thermal springs from Karlovy Vary, Czech Republic. *Phytotaxa* 181:279–92.
- Komárek, J. 2006. Cyanobacterial taxonomy: current problems and prospects for the integration of traditional and molecular approaches. *Algae* 21:349–75.
- Komárek, J. & Anagnostidis, K. 2005. Süßwasserflora von Mitteleuropa, bd. 19/2: Cyanoprokaryota: Oscillatoriales. *Spektrum Akademischer Verlag*, 19:1–759.
- Komárek, J., Kaštovsky, J., Mares, J. & Johansen, J. R. 2014. Taxonomic classification of Cyanoprokaryotes (cyanobacterial genera) 2014, using a polyphasic approach. *Preslia* 86:295–335.
- Konstantinou, D., Voultsiadou, E., Panteris, E., Zervou, S. K., Hiskia, A. & Gkelis, S. 2019. *Leptothoe*, a new genus of marine cyanobacteria (Synechococcales) and three new species associated with sponges from the Aegean Sea. *J. Phycol.* 55:882–97.
- Kremer, B., Kazmierczak, J. & Stal, L. J. 2008. Calcium carbonate precipitation in cyanobacterial mats from sandy tidal flats of the North Sea. *Geobiol.* 6:46–56.
- Kumar, S., Stecher, G., Li, M., Knyaz, C. & Tamura, K. 2018. MEGA X: molecular evolutionary genetics analysis across computing platforms. *Mol. Biol. Evol.* 35:1547–9.
- Langhans, T. M., Storm, C. & Schwabe, A. 2009. Community assembly of biological soil crusts of different successional stages in a temperate sand ecosystem, as assessed by direct determination and enrichment techniques. *Microb. Ecol.* 58:394–407.
- Lehnert, L. W., Thies, B., Trachte, K., Achilles, S., Osses, P., Baumann, K., Schmidt, J. et al. 2018. A case study on fog/low stratus occurrence at Las Lomitas, Atacama Desert (Chile) as a water source for biological soil crusts. *Aerosol Air Qual. Res.* 18:254–69.
- Marin, B., Nowack, E. C. & Melkonian, M. 2005. A plastid in the making: evidence for a second primary endosymbiosis. *Protist* 156:425–32.
- Martínez, A. & Asencio, A. D. 2010. Distribution of cyanobacteria at the Galeda cave (Spain) by physical parameters. *J. Caves Karst Stud.* 72:11–20.
- Mikhailyuk, T. I., Vinogradova, O. N., Glaser, K. & Karsten, U. 2016. New taxa for the flora of Ukraine, in the context of modern approaches to taxonomy of Cyanoprokaryota/Cyanobacteria. *Int. J. Algae* 18:301–20.
- Miller, S. R., Castenholz, R. W. & Pedersen, D. 2007. Phylogeography of the thermophilic cyanobacterium *Mastigocladus laminosus*. *J. Appl. Environ. Microbiol.* 73:4751–9.
- Miscoe, L. H., Johansen, J. R., Kociolek, J. P., Lowe, R. L., Vaccarino, M. A., Pietrasiak, N. & Sherwood, A. R. 2016. The diatom flora and cyanobacteria from caves on Kauai, Hawaii. *Acta Bot. Hungarica* 58:3–4.
- Mühlsteinová, R., Johansen, J. R., Pietrasiak, N. & Martin, M. P. 2014. Polyphasic characterization of *Kastovskya adunca* gen. nov. et comb. nov. (Cyanobacteria: Oscillatoriales), from desert soils of the Atacama Desert, Chile. *Phytotaxa* 163:216–28.
- Neustupa, J. & Škaloud, P. 2008. Diversity of subaerial algae and cyanobacteria on tree bark in tropical mountain habitats. *Biologia* 63:806–12.
- Osorio-Santos, K., Pietrasiak, N., Bohunická, M., Miscoe, L. H., Kováčik, L., Martin, M. P. & Johansen, J. R. 2014. Seven new species of *Oculatella* (Pseudanabaenales, Cyanobacteria): taxonomically recognizing cryptic diversification. *Eur. J. Phycol.* 49:450–70.
- Pessi, I. S., Lara, Y., Durieu, B., Maalouf, P. D. C., Verleyen, E. & Wilmotte, A. 2018. Community structure and distribution of benthic cyanobacteria in Antarctic lacustrine microbial mats. *FEMS Microbiol. Ecol.* 94:fy042.
- Petersen, J. B. 1923. Freshwater *Cyanophyceae* of Iceland. *Botany of Iceland* 2:249–324.
- Rigonato, J., Gama, W. A., Alvarenga, D. O., Branco, L. H. Z., Brandini, F. P., Genuario, D. B. & Fiore, M. F. 2016. *Aliterella atlantica* gen. nov., sp. nov., and *Aliterella antarctica* sp. nov., novel members of coccoid Cyanobacteria. *Int. J. Syst. Evol. Microbiol.* 66:2853–61.
- Robinson, C., Gibbes, B., Carey, H. & Li, L. 2007. Salt-freshwater dynamics in a subterranean estuary over a spring-neap tidal cycle. *J. Geophys. Res. Oceans* 112:1–15.
- Ronquist, F. & Huelsenbeck, J. P. 2003. MrBayes 3: Bayesian phylogenetic inference under mixed models. *Bioinformatics* 19:1572–4.
- Shalygin, S., Huang, I. S., Allen, E. H., Burkholder, J. M. & Zimba, P. V. 2019. *Odorella benthamica* gen. & sp. nov. (Pleurocapsales, Cyanobacteria): an odor and prolific toxin producer isolated from a California aqueduct. *J. Phycol.* 55:509–20.
- Stackebrandt, E. 2006. Taxonomic parameters revisited: tarnished gold standards. *Microbiol. Today* 33:152–5.
- Stackebrandt, E. & Goebel, B. M. 1994. Taxonomic note: a place for DNA-DNA reassociation and 16S rRNA sequence analysis in the present species definition in bacteriology. *Int. J. Syst. Evol. Microbiol.* 44:846–9.
- Stanier, R. Y., Kunisawa, R., Mandel, M. & Cohen-Bazire, G. 1971. Purification and properties of unicellular blue-green algae (Order *Chroococcales*). *Bacteriol. Rev.* 35:171–205.
- Strunecký, O., Elster, J. & Komárek, J. 2011. Taxonomic revision of the freshwater cyanobacterium “*Phormidium*” *murrayi* Wil-mottia murrayi. *Fottea* 11:57–71.
- Taton, A., Grubisic, S., Brambilla, E., De Wit, R. & Wilmotte, A. 2003. Cyanobacterial diversity in natural and artificial

- microbial mats of Lake Fryxell (McMurdo Dry Valleys, Antarctica): a morphological and molecular approach. *App. Environ. Microbiol.* 69:5157–69.
- Turland, N. J., Wiersma, J. H., Barrie, F. R., Greuter, W., Hawksworth, D. L., Herendeen, P. S., Knapp, S. et al. 2018. *International Code of Nomenclature for Algae, Fungi, and Plants (Shenzhen Code) Adopted by the Nineteenth International Botanical Congress Shenzhen, China, July 2017. Regnum Vegetabile 159.* Koeltz Botanical Books, Glashütten, Germany. DOI: <https://doi.org/10.12705/Code.2018>.
- Vinogradova, O., Mikhailyuk, T., Glaser, K., Holzinger, A. & Karsten, U. 2017. New species of *Oculatella* (Synchococcales, Cyanobacteria) from terrestrial habitats of Ukraine. *Ukr. Bot. J.* 74:509–20.
- Vazquez-Martinez, J., GUTIERREZ-VILLAGOMEZ, J. M., Fonseca-García, C., Ramirez-Chavez, E., MONDRAGON-SANCHEZ, M. L., Partida-Martinez, L., ... & Molina-Torres, J. (2018). *Nodosilinea chupicuarens* sp. nov. (Leptolyngbyaceae, Synchococcales) a subaerial cyanobacterium isolated from a stone monument in central Mexico. *Phytotaxa* 334:167–182.
- Wang, Y., Cai, F., Jia, N. & Li, R. 2019. Description of a novel coccoid cyanobacterial genus and species *Sinocapsa zengkensis* gen. nov. sp. nov. (Sinocapsaceae, incertae sedis), with taxonomic notes on genera in Chroococcidiopsidales. *Phytotaxa* 409:146–60.
- Whitton, B. A. 2012. *Ecology of Cyanobacteria II: Their Diversity in Space and Time*. Springer Science & Business Media, pp. 90–127.
- Williams, L., Borchhardt, N., Colesie, C., Baum, C., Komsic-Buchmann, K., Rippin, M., Becker, B., Karsten, U. & Büdel, B. 2017. Biological soil crusts of Arctic Svalbard and of Livingston Island, Antarctica. *Polar Biol.* 40:399–411.
- Wilmotte, A., Van der Auwera, G. & De Wachter, R. 1993. Structure of the 16 S ribosomal RNA of the thermophilic cyanobacterium *Chlorogloeopsis* HTF (“*Mastigocladus laminosus* HTF”) strain PCC7518, and phylogenetic analysis. *FEBS Lett.* 317:96–100.
- Zammit, G., Billi, D. & Albertano, P. 2012. The subaerophytic cyanobacterium *Oculatella subterranea* (Oscillatoriales, Cyanophyceae) gen. et sp. nov.: a cytomorphological and molecular description. *Eur. J. Phycol.* 47:341–54.
- Zammit, G., Billi, D., Shubert, E., Kaštokský, J. & Albertano, P. 2011. The biodiversity of subaerophytic phototrophic biofilms from Maltese hypogea. *Fottea* 11:187–201.
- Zammit, G., De Leo, F., Albertano, P. & Urzì, C. 2008a. A preliminary comparative study of microbial communities colonizing ochre-decorated chambers at the Hal Saflieni Hypogeum at Paola, Malta. In *Proceedings of the 11th International Congress on Stone Deterioration Nicolaus Copernicus University Press, Torun*, pp. 555–562.
- Zammit, G., Psaila, P. & Albertano, P. 2008b. An investigation into biodeterioration caused by microbial communities colonising artworks in three maltese palaeo-christian catacombs. In *Proceedings of the 9th International Conference on NDT of Art, Jerusalem*, pp. 25–30.
- Zhang, Q., Zheng, L., Li, T., Li, R. & Song, L. 2018. *Aliterella shaanxiensis* (Aliterellaceae), a new coccoid cyanobacterial species from China. *Phytotaxa* 374:211–20.
- Zuker, M. (2003). Mfold web server for nucleic acid folding and hybridization prediction. *Nucleic acids research* 31:3406–3415.

### Supporting Information

Additional Supporting Information may be found in the online version of this article at the publisher's web site:

**Table S1.** 16S rRNA gene sequence similarities among *Cyanocohniella* strains.

**Table S2.** Percent dissimilarity (100 × uncorrected p-distance) among aligned 16S–23S ITS regions of *Cyanocohniella* species.

**Table S3.** 16S rRNA gene sequence similarities among *Oculatella* strains.

**Table S4.** Percent dissimilarity (100 × uncorrected p-distance) among aligned 16S–23S ITS regions of *Oculatella* species.

**Table S5.** 16S rRNA gene sequence similarities among four *Aliterella* strains and their relatives.

**Table S6.** Percent dissimilarity (100 × uncorrected p-distance) among aligned 16S–23S ITS regions of *Aliterella* species.